
STREAMING SINGULAR VALUE DECOMPOSITION FOR BIG DATA APPLICATIONS

A PREPRINT

Gurpreet Singh^{†1}, Soumyajit Gupta^{†2}, Matthew Lease³ and Clint Dawson⁴

²Department of Computer Science

³School of Information

⁴Oden Institute for Computational Engineering and Sciences

¹The University of Texas at Austin

{gurpreet, smjtgupta, ml}@utexas.edu, clint.dawson@oden.utexas.edu

March 4, 2021

ABSTRACT

Singular Value Decomposition (SVD) plays a pivotal role in exploratory data analysis. However, in a Big Data setting computing the dominant singular vectors is often restrictive due to the main memory requirements imposed by the dataset. Recently introduced randomized projection schemes attempt to mitigate this memory load by constructing approximate projections of the true dataset in a streaming setting. However, these projection methods come at the cost of approximation errors in both top singular values and vectors. Furthermore, in order to bound the approximation error, an over-sampled projection is required, often much larger in dimension than the desired rank. This latter consideration can still be memory intensive when the data dimension is large or extraneous when the desired rank approximation is close to the full rank. We present a two stage neural optimization approach as an alternative to conventional and randomized SVD techniques, where the memory requirement depends explicitly on the feature dimension and desired rank, independent of the sample size. The proposed scheme reads data samples in a streaming setting with the network minimization problem converging to a low rank approximation with high precision. Our architecture is fully interpretable where all the network outputs and weights have a specific meaning. We evaluate our results on various performance metrics against state of the art streaming methods. We also present numerical experiments for Singular and Eigen value decomposition on real data at various scales to show the memory efficiency of our proposed approach.

Keywords SVD, Eigen, Interpretable, Neural Nets, High-Precision, Big Data

1 Introduction

Singular and Eigen value decompositions are pivotal to exploratory data analysis in identifying an invariant structure under a minimalistic representation (assumptions on the structure). The core objective is to identify Singular or Eigen directions that are invariant under transformation eluding the span (or volume) of resolvable information contained in the dataset. Singular Value Decomposition (SVD) serves as a front line data analysis tool unraveling both long and short range correlations in the sample and feature dimensions. With the advent of digital sensors and modern day data acquisition technologies the sheer amount of data now requires that we revisit the solution scheme with reduced memory consumption as the target. In Big Data Applications, the primary objective is to identify the top r -ranks (singular or eigen values) invariant directions that carry the most amount of information. This restriction on the feature dimension

[†]contributed equally

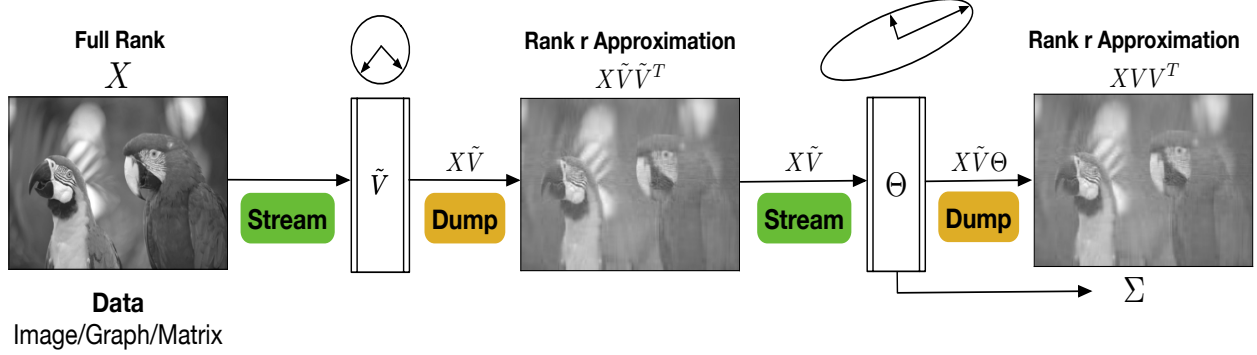


Figure 1: An overview of the low-memory, two-stage Neural SVD solver for Big Data Applications. Stage 1 identifies the span of the desired rank- r approximation. Stage 2 rotates this span to align with the singular vectors while extracting the singular values of the data. The input data can either be streamed row-wise from a server or secondary memory.

mitigates the processing load however, the large number of samples still pose an issue. In this work, we attempt to reformulate one of the most prominent data analysis tools (SVD) with special emphasis on the main memory load requirement that precludes its use in Big Data setting. Natural data matrices have a decaying spectrum wherein saving the data in memory in its original form is often redundant. A necessary task to avoid this redundancy is to find low rank factors that effectively represent the data. Finding such a low rank approximation is a fundamental task in numerous applications including Image Compression [1], Image Recovery [2], Background Removal [3], Recommendation Systems [4] and also used as a pre-processing step for Clustering [5] and Classification [6]. Due to the massive size of data in modern applications, it is often not possible to load the entire data matrix into the main memory resulting in a bottleneck for conventional solvers.

Randomized projections of the data matrix load a low-rank sketch of the dataset to circumvent this issue. The central idea in such projection based schemes is that the sketch be of minimum size as well as retain most of the information content of the original data. The first one-pass algorithm based on random projections appear in Woolfe et al. [7]. Since then, there are a number of highly cited works in Halko et al. [8], Woodruff [9], Boutsidis et al. [10], Upadhyay [11] *etc.* One of the most recent works, SketchySVD [12] is shown to provide consistent approximations compared to its predecessors with tight bounds. However, for a limited memory environment the hyper-parameters of sketching algorithms must be chosen to be optimal. The size or chunk of the data matrix to be streamed and subsequently processed is dependent on the memory capacity of the processing machine. Reading too many samples or large vectors, while preserving only low-dimensional projections to satisfy memory constraints diminish the expected accuracy. Optimal memory-accuracy-speed trade-offs need to be achieved during stream processing of large scale big-data in limited memory settings. Given a fixed chunk of data, the way it is loaded into memory also proves to be a bottleneck in subsequent processing. These issues have not been comprehensively addressed in prior works, and is the focus of this paper in an attempt to achieve practical stream processing algorithms for big-data applications.

We present a low-weight neural optimization alternative to SVD where the memory requirement depends only on the number of features (n) and the desired rank (r) while remaining independent of the number of samples (m). Our approach relies upon the Eckart-Young-Mirsky theorem which states that for a rank- r approximation, minimizing tail energy ($n - r$ non-trivial and orthogonal invariant directions) in Frobenius norm aligns the top r invariant directions to span a rank- r basis while maximizing the rank- r energy. Since the total energy of the system is constant (data is not being added or removed), the fixed point of this minimization problem corresponds to a rank- r approximation. Our numerical experiments demonstrate that the difference in tail energies (Frobenius norm) obtained using our approach and conventional SVD achieves a machine precision zero while keeping the memory requirement low. The main application thrust of our work is to allow an energy efficient ranking or re-ranking of the dataset under a streaming setting. Further, our two-stage framework provides the user flexibility when either a rank- r approximation (stage 1) or both rank- r approximation with singular vectors and values (stage 2) as desired. In the event of the first choice, the second stage of our framework can be discarded to lower the overall computational cost. Our contributions in this work are as follows:

- A simple data and representation driven neural SVD solver to compute rank- r singular vectors and values.
- A streaming neural architecture for big data applications with low main memory (RAM) requirement.
- The proposed network minimization problem generates GPU bit precision results.

- The proposed architecture is fully interpretable and verifiable (tight error bounds) where all the network weights and layer outputs have a specific meaning.
- Our proposed approach can be trivially modified to perform Eigen decomposition and Principal Component Analysis.
- We will provide full access to data and source code for reproducibility upon acceptance.

2 Motivation

In the recent years, we are experiencing an exponential increase in the availability of high quality (high SNR) time evolving satellite image data for natural and artificial processes. Here, identifying long range, time-periodic structures will directly lead to improvements in several areas including but not limited to environmental impact assessment, Geo-sciences, planetary scale phenomena identification, and resource management. SVD is our closest ally and the most prominent tool in identifying the dominant features of a dataset when addressing this challenge. In an attempt to further this pursuit, our high precision neural SVD solver draws upon three seminal works in the field of large-scale matrix decomposition:

1. Sanger [13] presented a simple neural network to approximate the relationship between the input and output of a linear transmission channel. Here, the system was represented as a chain of linear transformations using two approximation methods. This method inspired our low-weight network design where the invariants: right singular vectors and values are extracted as network weights.
2. Tropp et al. [12] presented SketchySVD as the first randomized SVD algorithm to work under a streaming setting for big data applications. SketchySVD projects the original data to form row, column and core sketches followed by a low rank SVD approximation. This work provided us with a unique perspective and challenge in reformulating algorithms to suit the needs of data streaming modalities.
3. Haidar et al. [14] presented an out-of-memory block SVD solver that computes the top singular values and vectors in a block fashion, iteratively. The second stage of our algorithm borrows upon by this concept to compute singular values in a block-wise manner.

3 Notation

As per the standard notation in literature, let us denote the raw data matrix as $X \in \mathbb{R}^{m \times n}$ and its approximation as \hat{X} . Let its rank r truncation be X_r , where where in a big data setting let us assume that the rank is significantly lower than the both dimensions ($r \ll \min(m, n)$). Let $X_r = U_r \Sigma_r V_r^T$ be its Singular Value Decomposition (SVD) and let $X^T X = V \Lambda V^T$ be its Eigen Decomposition. Correspondingly, $U \in \mathbb{R}^{m \times r} = [u_1, \dots, u_r]$ and $V \in \mathbb{R}^{n \times r} = [v_1, \dots, v_r]$ are its left and right singular vectors respectively, and $\Sigma \in \mathbb{R}^{r \times r} = \text{diag}(\sigma_1, \dots, \sigma_r)$ and $\Lambda \in \mathbb{R}^{r \times r} = \text{diag}(\lambda_1, \dots, \lambda_r)$ are its singular and eigen values respectively.

4 Related Works

Sketching based algorithms rely on Random projections. The goal is to load a sketch of the original matrix, that is small memory-wise while preserving important properties of the original space. One of the earliest works include Gaussian Random Projection matrices based on the Johnson-Lindenstrauss [15] lemma and Subsampled Randomized Hadamard Transform (SRHT) [9]. Both of these methods involve loading the entire data into memory, forming the projection matrix and then computing the sketch. Count Sketch based projection [16] overcomes this by directly computing the sketch without loading the entire data.

The core idea of randomized decomposition approaches is to make one or two passes over the data and compute efficient sketches. They can be broadly categorized into four main branches: Sampling based methods (Subset Selection [17] and Randomized CUR [18]), Random Projection based QR [8], Randomized SVD [8] and Nyström Methods [19]. The sketches can represent any combination of row space, column space or the space generated by the intersection of rows and columns (core space). However, these approaches are limited by their requirement to load the entire dataset in memory.

Due to restrictions on localized storage cost, streaming algorithms are becoming popular to achieve matrix decomposition under low-rank setting. SketchySVD [12] provides the first randomized method to work under streaming setting for big data, and to the best of our knowledge is the only such method till date. The algorithm is stated in **Alg. 1**. It works by computing overestimates of the required rank, building projection matrices of overestimated rank, and taking row,

column and core space projection. QR decomposition on the row and column matrices give as estimate of the left and right singular vectors. SVD is performed on the core matrix to estimate the singular values. Finally, the singular values and vectors are returned after projecting them back to the original row and column dimension. The time complexity of the algorithm is $O(k^2(m+n))$ with storage cost $O(k(m+n))$, where $k = 4r + 1$.

5 Network Architecture

The proposed network architecture is divided into two stages: (1) Projection, and (2) Rotation, each containing only one layer of linear activation functions with no bias. Fig. 2 shows an outline of the this two-stage network architecture where all the weights and outputs have a specific meaning enforced using representation and data driven loss terms.

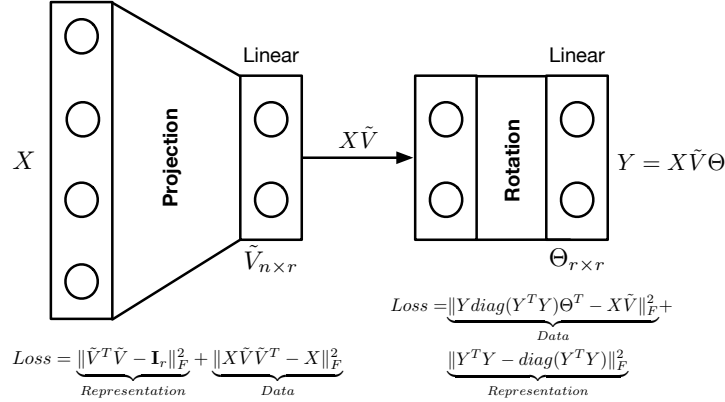


Figure 2: Network Architecture: Projection (Net1) and Rotation (Net2) for a 2 stage SVD

Stage 1: Rank- r Sub-space Identification: The projection stage constructs an orthonormal basis that spans the r -dimensional sub-space of the full feature dimensional (n) space. This orthonormal basis ($\tilde{V}_{n \times r}$) is extracted as the stage-1 network weights once the network minimization problem converges to a fixed-point. The representation loss ($\tilde{V}^T \tilde{V} - \mathbf{I}_r$) in stage-1 enforces the orthonormal requirement on the projection space (even in a low rank setting) while the data-driven loss ($X \tilde{V} \tilde{V}^T - X$) minimizes the tail energy. Please note that these orthonormal vectors \tilde{V} are not the singular vectors V , but a rotated variant of those spanning the same rank- r subspace.

Stage 2: Singular Value and Vector Extraction: The rotation stage then extracts the singular values by rotating the orthonormal vectors ($\tilde{V}_{n \times r}$) to align with the right singular vectors ($V = \tilde{V} \Theta$). As before, the representation loss ($Y^T Y - \text{diag}(Y^T Y)$) ensures a rotation such that $Y^T Y$ is a diagonal matrix containing the eigenvalues. The data driven loss ($Y \text{diag}(Y^T Y) \Theta^T - X \tilde{V}$) minimizes the loss of energy under this rotation. As discussed later in **Section 5.2**, this choice of loss terms equipped with a Frobenius norm ensures a rank- r approximation in accord with the Eckart-Young-Mirsky (EYM) theorem. We are therefore able to preemptively state that the expected values of the stage-1 loss term at the minimum must correspond to the rank ($n - r$) tail energy. This can be verified by performing a full SVD using conventional solvers and computing a Frobenius norm on a reconstruction of the data using the bottom ($n - r$) singular values and vectors or alternatively by computing ($\|A - A_r\|_F$). Further, the second loss term is expected to reach a machine precision zero at the minimum. A rough sketch can be generated from **Stage 1** or projection step of our proposed neural SVD solver by enforcing a looser termination criteria on the loss function. This will result in lesser number of passes required over the data matrix resulting in reduced compute time at the cost of solution accuracy.

Once, the network minimization problem converges, the singular values are extracted from **Stage 2** network weights Θ as $\Sigma_r^2 = \Theta^T \Theta$. The right singular vectors can now be extracted using **Stage 1** and **Stage 2** layer weights given by $V_r = \tilde{V} \Theta / \text{diag}(\Theta^T \Theta)$. Once V_r and Σ_r are known, left singular vectors $U_r = (X \tilde{V} \tilde{V}^T) V_r \Sigma_r^{-1}$. Here, $(X \tilde{V} \tilde{V}^T)$ is the rank- r approximation from **Stage 1** dumped into the secondary memory.

5.1 Data Streaming

Given the data matrix $A^{m \times n}$, we stream the data along the dimension that is lower, since $r < \min(m, n)$. Assuming the data matrix has m samples and n features, where $m > n$, we stream the feature vector of samples in batches. This lets us construct a network with the minimal weights as possible for a rank r approximation. We use the built-in Keras

fit_generator class to stream the data for our network. Since in a big data setting, we cannot ever load the entire data into memory, we assume the actual data to reside in some server or the secondary memory (HDD). Thus, given a pointer to the data, the function yields a batch of specified size for the network to train on for specific epochs. This ability saves main memory load and allows us to process bigger datasets than reported in previous works. Note that for the first network to converge, we expect multiple passes over the original data. For Stage 1, the input data is assumed to be streamed from an external source. The output data is dumped onto the secondary memory assuming a low rank approximation is still main memory intensive. For Stage 2, this low rank approximation in the secondary memory is streamed as input, and the corresponding Singular Values are saved in main memory.

5.2 Error Bounds

In the following, we present error bounds for the two-stage neural optimization problem following Eckart-Young-Mirsky (EYM) theorem equipped with Frobenius norm.

Stage 1: From EYM theorem [20, 21], we have that for any rank- r matrix B_r of X , the tail energy $\|X - B_r\|_F$ in Frobenius norm $\|\cdot\|_F$ is bounded below by,

$$\|X - B_r\|_F \geq \|X - X_r\|_F, \quad (1)$$

where, X_r is the rank- r approximation of X . The equality holds true only when $B_r = X_r$. Let us consider a matrix $\tilde{V}_{n \times r}$ of r orthonormal vectors $\tilde{v}_{i=1,2,\dots,r}$ such that,

$$\tilde{V}^T \tilde{V} = \mathbf{I}_r. \quad (2)$$

We now define any rank- r approximation B_r as,

$$B_r = X \tilde{V} \tilde{V}^T$$

Substituting this in Eq. 1 we get,

$$\|X - X \tilde{V} \tilde{V}^T\|_F \geq \|X - X_r\|_F.$$

The minimization problem under the equality constraint Eq. 2 then reads,

$$\min_{\tilde{V}} \|X - X \tilde{V} \tilde{V}^T\|_F \quad s.t. \quad \tilde{V}^T \tilde{V} = \mathbf{I}_r \quad (3)$$

with a minimum at the fixed point $\tilde{V}_* = \text{span}\{v_1, v_2, \dots, v_r\}$ where $v_{i=1,2,\dots,r}$ are the right singular eigenvectors of X_r . This minimization problem (Eq. 3) describes the Stage 1 loss function of our network architecture.

Stage 2: From the fixed point of the previous minimization problem Eq. 1 we also have $\tilde{V}_* \tilde{V}_*^T = V_r V_r^T$. According to the EYM theorem the tail energy with respect to rank- r approximation is,

$$\begin{aligned} \|X_r - X(\tilde{V}_* \theta)(\tilde{V}_* \theta)^T\|_F &\geq 0 \\ \|X V_r V_r^T - X(\tilde{V}_* \theta)(\tilde{V}_* \theta)^T\|_F &\geq 0 \\ \|X\|_F \|V_r V_r^T - (\tilde{V}_* \theta)(\tilde{V}_* \theta)^T\|_F &\geq 0 \end{aligned}$$

where the equality holds true when $\theta \theta^T = \mathbf{I}_r$. In other words, any rotation θ_r out of the hyper-plane of the rank- r subspace of X_r will increase the tail energy. If $V_r = [v_1, v_2, \dots, v_r]$, where $v_{i=1,2,\dots,r}$ are the right singular eigenvectors of X_r we have,

$$(X V_r)^T (X V_r) = V_r^T (X^T X) V_r = \Sigma_r. \quad (4)$$

Following Eq. 4 let us define,

$$(X V_* \theta)^T (X V_* \theta) = \tilde{\Sigma}_r. \quad (5)$$

Subtracting Σ_r from both sides of Eq. 5 and taking a Frobenius norm we have,

$$\|(X \tilde{V}_* \theta)^T (X \tilde{V}_* \theta) - \Sigma_r\|_F = \|\tilde{\Sigma}_r - \Sigma_r\|_F \geq 0$$

with the minimum achieved when $\tilde{V}_* \theta = V_r$. Assuming $Y = X \tilde{V}_* \theta$ for convenience of notation, the minimization problem now reads:

$$\begin{aligned} \min_{\theta} \quad & \|Y \theta^T - X \tilde{V}_*\|_F \\ s.t. \quad & \theta^T \theta = \mathbf{I}_r \text{ and } Y^T Y - \text{diag}(Y^T Y) = 0 \end{aligned}$$

5.3 Network Interpretability

As described before in Fig. 2, our network weights and outputs are strictly defined and incorporated as losses in the network minimization problem. In order to create a distinction, we refer to the problem informed (SVD) restrictions on the network weights as representation driven losses. This is in contrast to kernel regularization loss often considered to impose a weak requirement on the network weights to be small. The representation driven, orthonormality loss term, in Stage 1 enforces that the weights \tilde{V} must span a rank- r subspace or ($\tilde{V}^T \tilde{V} = \mathbf{I}_r$). This additional loss term ensures that vectors \tilde{V} are orthonormal even when the desired rank- r system itself is low rank. We numerically verify the interpretability of the layer outputs and weights by considering two networks: (1) with, and (2) without the aforementioned orthonormality loss.

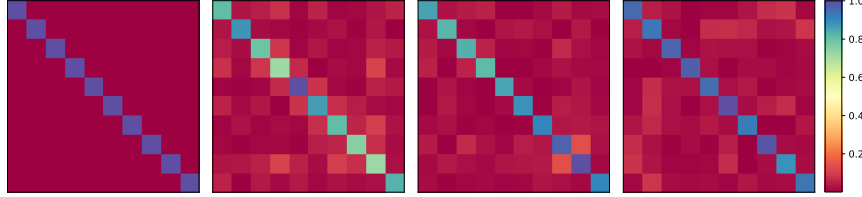


Figure 3: Synthetic Low Rank Scenario: Correlation Map of extracted vectors \tilde{V} over four runs. Orthonormality is imposed for the first run resulting in a diagonal structure. Absence of this condition results in a scatter, as expected.

For the first case, we consider a synthetic data matrix $X_{15 \times 15}$ where the top 5 singular values are positive while the rest are zero. The objective is to extract the top 10 singular vectors where the desired rank is higher than the rank of the system itself. A total of four training runs are considered: one run for a network with the orthonormality condition imposed and three runs for another network without this additional requirement. **Fig. 3** shows the correlation map between the recovered vectors \tilde{V} for each of the four runs. Notice that only when the orthonormality criteria is not imposed, we get scatter away from the diagonal matrix, although all four runs converged to the same tail energy. Since the true rank of X is 5, the null space of X is of dimension 10. The absence of this orthonormality imposing, representation loss results in non-orthonormal vectors \tilde{V} spanning the low-rank range space.

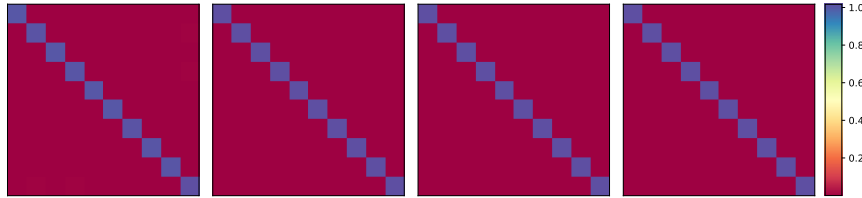


Figure 4: Synthetic Full Rank Scenario: Correlation Map of extracted vectors \tilde{V} over four runs. Orthonormality loss now does not contribute and therefore all runs have a diagonal structure.

For the second case, we consider a full-rank, synthetic data matrix $X_{15 \times 15}$. As before, we extract the top 10 singular vectors using four training runs: one with and three without imposing the orthonormality loss. Since the desired rank 10 system now itself is full rank, this additional loss term does not contribute, as expected. **Fig. 4** shows that the extracted vectors \tilde{V} remain orthonormal, for all the four runs, so as to minimize tail energy ($\|X(\tilde{V}\tilde{V}^T - \mathbf{I})\|_F$), as described in **Section 5.2** above. In fact, for any rank r approximation of a rank f system such that $r \leq f$, an arbitrary non-orthonormal matrix \tilde{V} will increase the tail energy and hence will not be a fixed point (solution) of our network minimization problem.

6 Results

We begin this section by first defining a few metrics for comparison and bench-marking purposes. In the subsequent subsections, we present our training setup, results and analysis for various synthetic and real datasets, which vary in scale from small to big data. Please note that our numerical results do not show variations over multiple runs due to a low-weight architecture. For all of the following numerical experiments, the **Stage 1** of our neural SVD solver requires at most 5 passes over the data matrix to converge.

6.1 Metrics

For comparison of the proposed solution vs. established methods and ground truth, we use the following error metrics, where A, \hat{A} represents the true and the reconstructed data matrices.

- **Scree Error:** Absolute values of the difference between singular values from our proposed approach and rank- r SVD.

$$scree_{err}(r) = |\sigma_i(A) - \hat{\sigma}_i(\hat{A})| \quad \forall i \in [1, r]$$

- **Trace Error:** Sum of the differences in the top- r singular values using our proposed approach and SVD.

$$trace_{err}(r) = \sum_{i=1}^r |\sigma_i(A) - \hat{\sigma}_i(\hat{A})|$$

- **Reconstruction Error:** Frobenius norm of the element wise error of the true data and its rank- r approximation.

$$frob_{err}(r) = \|A - \hat{A}\|_F^2 - \|A - A_r\|_F^2$$

- **Spectral Error:** 2 norm of the singular value of the true data and its rank- r approximation.

$$spectral_{err}(r) = \|A - \hat{A}\|_2 - \|A - A_r\|_2$$

- **Chi Square Statistic:** Deviation of the network recovered singular vectors from the true singular-vectors.

$$\chi^2_{err}(r) = 1 - \frac{1}{r} \|Corr(v_{[r]}(A), \hat{v}_{[r]}(\hat{A}))\|_F$$

Under perfect recovery, all the error metrics is expected to approximately achieve zero at machine precision. All of our numerical experiments were performed on a GPU using single (32-bit) precision floating point operations. Therefore, the tail energies are expected to be correct to upto 8 significant digits approximately in all the subsequent calculations.

6.2 Setup and Training

All experiments were done on a setup with Nvidia 2060 RTX Super 8GB GPU, Intel Core i7-9700F 3.0GHz 8-core CPU and 16GB DDR4 memory. We use Keras [22] library running on a Tensorflow 1.14 backend with Python 3.7 to train the networks presented in this paper. For optimization, we use AdaMax [23] with parameters ($lr=0.001$) and 2000 steps per epoch. The batch-sizes vary with dataset sizes and are therefore not reported explicitly.

6.3 Storage Complexity Analysis

To get an estimate of the storage efficiency our network provides, lets us consider all the intermediate matrices that occupy the main memory (RAM) while the computations of U, Σ, V are being performed. Our Network has two layers, one corresponding to the low rank projections vectors $\tilde{V}_{r \times n}$ and the rotation matrix $\Theta_{r \times r}$. In Sketchy SVD, we have four projection matrices $\Gamma_{m \times k}, \Omega_{n \times k}, \Phi_{m \times s}, \Psi_{n \times s}$, three projected data matrices $Y_{m \times k}, X_{n \times k}, Z_{s \times s}$, and three rank- k decomposition $Q_{m \times k}, C_{k \times k}, P_{n \times k}$. Thus, the overall memory efficiency (s_{eff}) factor between Sketchy SVD and ours for a rank- r approximation is as follows:

$$\begin{aligned} s_{eff} &= \frac{\text{SketchySVD}}{\text{Ours}} \\ &= \frac{mk + nk + ns + ms + mk + nk + s^2 + mk + nk + k^2}{rn + r^2} \\ &= \frac{3(m+n)(k+s) + s^2 + k^2}{r(n+r)} \\ &\approx \frac{3(m+n)(4r+8r) + (8r)^2 + (4r)^2}{r(n+r)} \quad k = 4r+1, s = 2k+1 \\ &= \frac{36(m+n) + 80r}{(n+r)} \\ &\approx 2.3e3 \quad \text{for MNIST}(m = 60k, n = 784, r = 150) \end{aligned}$$

To validate the above ratio, we constructed a synthetic dataset of $m = 50000$ rows and the number of columns were varied starting at $n = 1000$ with increments of 1000. **Fig. 5** shows the log plot of the memory allocation (in Megabytes), where the storage efficiency of our method is evident and validates the number for MNIST example.

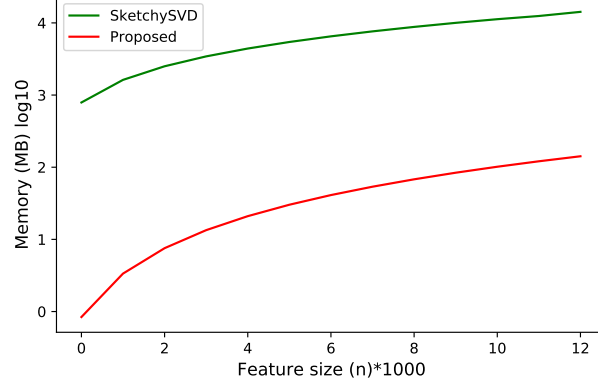


Figure 5: Storage Comparison

6.4 Natural Image: Parrots (SVD)



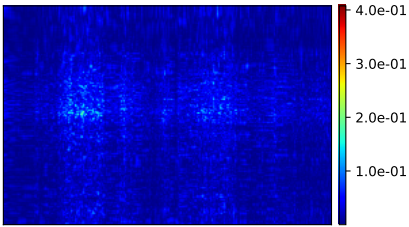
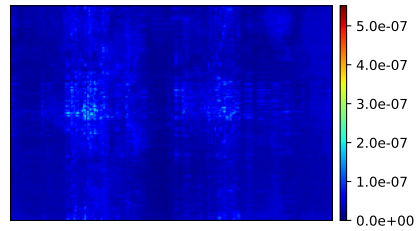
(a) True Image

(b) Rank $r = 20$ Truncation

(c) Sketchy SVD Reconstruction



(d) Our Reconstruction

(e) $|\hat{A}^{sketchy} - A_r|$ (f) $|\hat{A}^{net} - A_r|$ Figure 6: Rank $r=20$ Reconstruction for Parrot

As an example for SVD of natural images, we choose the well known Parrots image from the Image Processing domain. The original image is in RGB format, converted to a gray scale for demonstration purposes followed by normalization between $[0, 1]$. This 1024×1536 data matrix is then used to compute a rank $r = 20$ approximation for comparison and

numerical analysis. **Fig. 6** shows the result of the low rank reconstruction for truncated SVD, SketchySVD and our network. Visually one can verify that Fig. 6 (b,d) are similar while (c) is different. To make the error in approximation more clear, we plot the absolute difference of SketchySVD and our net from the truncated rank image. Fig. 6 (e,f) shows the the corresponding plots with heatmaps imposed for clarity. Notice that while the relative error for our network ($\sim 10^{-7}$) is close to the GPU precision, SketchySVD has significantly higher error scale (10^{-1}), validating the artifacts in the approximated image.

Table 1: Metric Performance of SketchySVD vs. Proposed

Method	rank	err_{tr}	err_{fr}	err_{sp}	χ_{err}^2
SketchySVD	r=10	17.939	27.904	18.071	0.492
Ours		0.0553	0.0	0.0	0.018
SketchySVD	r=20	13.103	11.974	2.201	0.662
Ours		0.0556	0	0	0.023
SketchySVD	r=50	3.756	2.772	0.181	0.762
Ours		0.0857	1.91e-7	0	0.027
SketchySVD	r=100	0.977	0.614	2.14e-2	0.923
Ours		0.1013	8.58e-7	4.42e-7	0.033

We tabulate all metric scores for SketchySVD and the proposed method on the same image for various ranks (10, 20, 50, 100) in **Table. 1**. One can easily notice that as the expected rank increases, SketchySVD’s performance keeps on deteriorating for the χ_{err}^2 metric, as it is only guaranteed high precision solution for only few top values, and rest spread their energy as evident from Fig. 7. Our method gives consistent low errors on all the metrics showing it accuracy in approximating the true SVD.

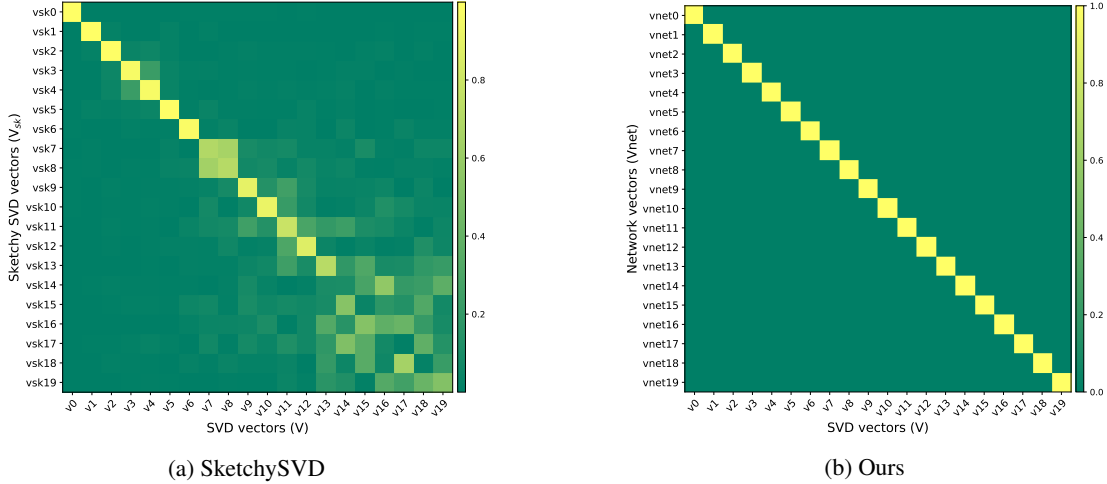


Figure 7: Correlation between true and predicted vectors

Another figure of interest that highlights the distinction in estimation accuracy is the correlation plot between the true and the recovered rank- r vectors. **Fig. 7** such plots for Sketchy SVD and our method *w.r.t.* the true SVD vectors (V), where for $r = 20$ Sketchy SVD is able to maintain perfect correlation only for the top 3 vectors, while rest of them are some linear combinations of the true vectors. The lower the vector index, the higher the spread, owing to the random Gaussian projections which were initially constructed that did not preserve orthogonality. Our method on the other hand has a good correlation with the true vectors, indicated by the solid diagonal and zero off-diagonal entries.

Fig. 8 shows the scree plot for both methods, which plots the absolute difference between the predicted and the true singular values for each index. Not only the scale of error fluctuates across the top $r = 20$ values, but also the scale of error is 1. Comparably, our method incurs significantly lower loss in all the top 4204 singular values ($4e - 3$).

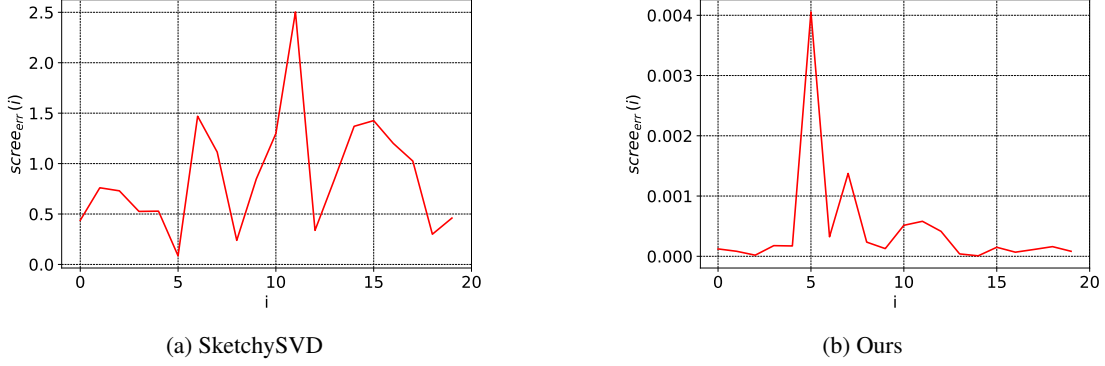


Figure 8: Scree Error for Parrot

6.5 Network Graph (SVD/Eigen)

Large scale network occurs in many applications where SVD is primarily used to identify the most important nodes or as a pre-processing step to community detection. For these kind of graph based datasets, we either perform SVD or Eigen decomposition on the graph, depending on the format in which the data arrives. We demonstrate results on the following graphs of varying size, tabulated in **Table. 2**. If the data arrives directly in the form of an adjacency matrix, we can perform SVD or Eigen decomposition on it directly. For cases, where an adjacency list is provided, a pre-processing step is required to convert the list representation in a sparse vector. Since Keras can handle sparse input data and sparse matrix operations, our method is trivially scalable to large sparse graphs. Since an Eigen decomposition problem is a special case of SVD, where the data matrix is symmetric positive semi-definite, our neural SVD solver is directly applicable.

Table 2: Description of the Network Graphs

	Nodes	Edges
Airlines [24]	235	2101
Twitter [24]	3556	188712
Wikivote [25]	8297	103689
Wikipedia [26]	49728	941425
Slashdot [25]	82168	948464

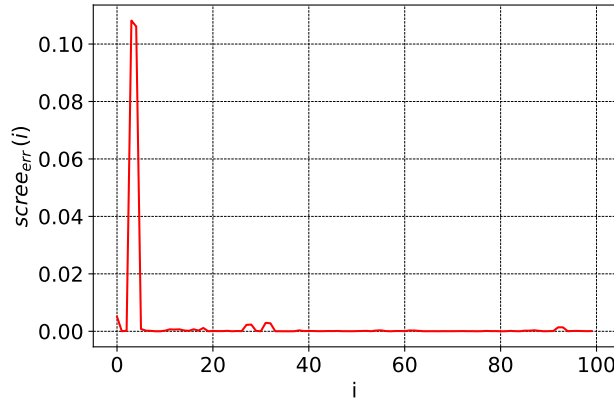


Figure 9: Scree Error for Slashdot Graph

The benchmark was generated for smaller graphs using a conventional SVD solver. For larger graphs, a similar benchmark was constructed using the *irlba* routine by Baglama and Reichel [27]. **Fig. 9** shows the scree plot for the Slashdot dataset. **Table. 3** shows the error metrics for all the graphs, where consistently low values are observed for Frobenius and Spectral error metrics.

Table 3: Metric Performance of Proposed method

Graph	rank	err_{tr}	err_{fr}	err_{sp}	χ_{err}^2
Airline	200	0.001	0	0	0.011
Twitter	200	0.022	0	0	0.014
Wikivote	200	0.029	0	0	0.027
Wikipedia	100	0.044	4.27e-6	1.23e-7	0.034
Slashdot	100	0.128	8.56e-6	6.92e-7	0.045

6.6 MNIST (PCA)

Principal Component Analysis (PCA) is a special variant of Eigen Decomposition, where the samples are mean corrected to center them before performing an Eigen decomposition. The MNIST dataset consists of images of handwritten digits, where each image is of size 28×28 with 60k images in the training set. To mold the dataset, we reshape each image into a 784-dim vector to obtain the data matrix $A_{60000 \times 784}$. In a streaming setting, the mean feature vector computation requires one pass over the data matrix. This can be subsequently used during the network training to mean correct streamed input vectors.

For MNIST data, it is known that $r = 200$ captures around 97%+ variance in the dataset. For SketchySVD, this would result in projection matrices of ranks $k = 4r + 1 = 801$ and $s = 2k + 1 = 1602$. Since MNIST data only has $n = 784$ features, this would result in extraneous computational load on the underlying conventional SVD solver. In this scenario, it is preferable to just perform full rank SVD on the dataset. **Table. 4** shows the error metrics under different rank setting.

Table 4: Metric Performance of the Proposed method

rank	err_{tr}	err_{fr}	err_{sp}	χ_{err}^2
20	0.071	0	0	0.012
50	0.092	0	0	0.025
100	0.122	1.45e-6	2.27e-7	0.052
200	0.154	3.08e-6	4.32e-7	0.071

6.7 Navier-Stokes Simulated Data (SVD)

For our next numerical experiment, we rely upon synthetic data generated using a Navier Stokes flow simulator for an incompressible fluid. The flow data is available on tensor-product grid on two-spatial and one temporal dimensions of size $(w, h, t) = (100 \times 50 \times 200)$. For each point on the grid, velocity vector values are available in both x and y spatial dimensions for 200 time instances. The fully-developed, flow pattern exhibits a periodicity in the time dimension at approximately every ~ 60 time step that can be identified using SVD as characteristic modes. The data is therefore reshaped into a spatial vector for each time instance resulting in a spatio-temporal matrix $A_{5000 \times 200}$. For comparison purposes, we use only the y -direction stream velocity.

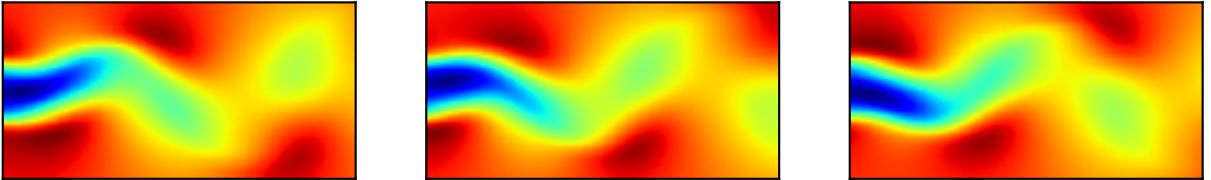
Figure 10: From left to right: x -direction stream velocity at times $t = 0, 100$, and 200

Fig. 10 shows the evolution of the stream velocity over three time instances and the inherent time-periodic nature of the data. Notice the central-left region of primary flow across all three images. **Fig. 11** shows the reshaped U vectors for the SketchySVD, True and our method. Notice that the image corresponding to the first left singular mode (also called dynamic modes) captures a notion of the primary flow in the left-center part. The second one captures spatial variations

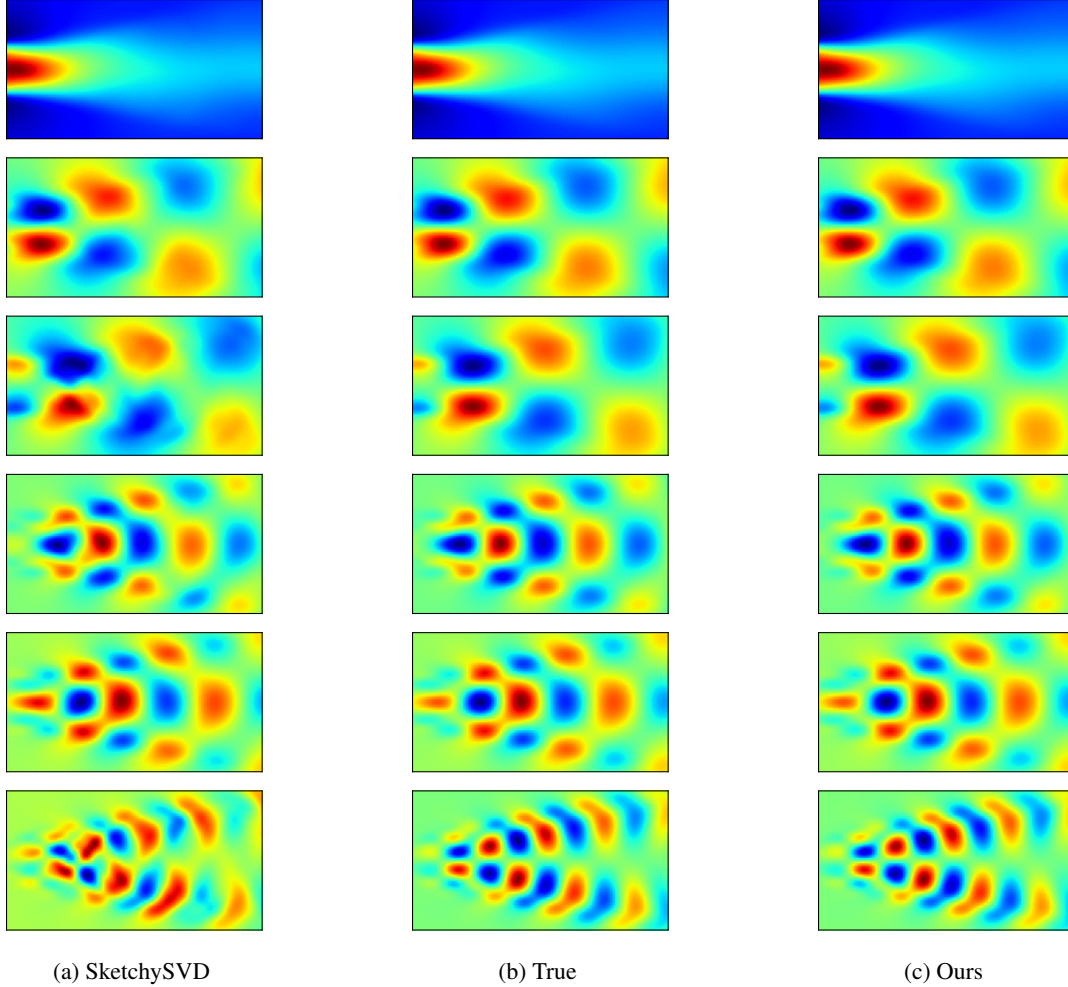


Figure 11: Reshaped U indicative of dynamic modes, corresponding to top six right singular vectors for $r = 6$. The dynamic modes of SketchySVD has visible errors at indices 2, 4, 5. Our proposed method does not have such artifacts.

of the flow as time progresses. For all the three methods, the first two modes are similar however, from the third mode onwards, SketchySVD starts deviating from the true solution. Our proposed approach, on the other hand is in good agreement with the true SVD solution. Note that our method computes the rank $r = 6$ approximation directly, wherein SketchySVD relies upon costly sketchy projections of ranks 25, 51 to arrive at the solution while incurring errors.

6.8 Hurricane Sandy Big Data (SVD)

Satellite data gathered by NASA for Hurricane Sandy over the Atlantic ocean represents the big data counter-part of Navier-Stokes simulation data. The data-set is openly available² and comprises of RGB snapshots captured at approximately one-minute interval. The full data-set consists of 896×719 pixel images for 1208 time-instances. For comparison purposes with conventional SVD solvers on a compute machine with 16 GB RAM, we truncate the data to an even 400×400 pixel image for the first 500 time-instances. Please note that this restriction is imposed by conventional and sketchy SVD methods due to their high main memory requirements. In contrast, our neural SVD solver can handle data sets that are orders of magnitude larger in size with the same hardware specification.

Fig. 12 shows evolution of Hurricane Sandy for two time instances. We would also like to point out that although the data matrices $A_{50k \times 50k}$ for network graph problem appears big, the non-zero entries are highly sparse. In comparison, the data matrix $A_{150k \times 500}$ for Hurricane Sandy is still big since the matrix itself is dense. Therefore, a benchmark case cannot be setup using **irlba** sparse SVD solver in this case. Similar to the Navier-Stokes simulation data, **Fig. 13** shows

²https://www.nasa.gov/mission_pages/hurricanes/archives/2012/h2012_Sandy.html

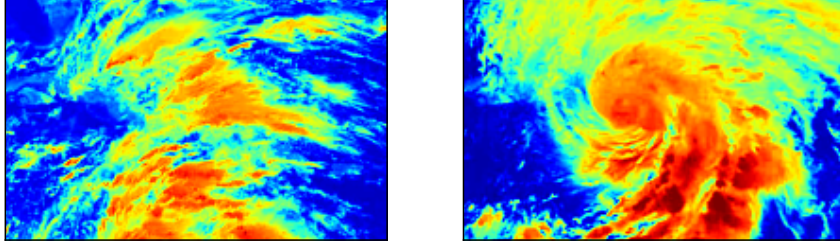


Figure 12: Satellite image captures of hurricane Sandy over the Atlantic ocean at $t = 0$ (left) and $t = 200$ minutes approximately (right)

three dynamic modes corresponding to rank 10, 50, 100 singular values. As shown, our results are in good agreement with conventional SVD whereas, Sketchy SVD shows substantial deviations after the first 50 dynamic modes. Here, we point out that accuracy is a matter of special concern in scientific computations. Any compression that results in substantial loss of information or obscuring an otherwise identifiable feature in recorded observations directly culls our capacity to make scientific improvements. Consequently, any exploratory data analysis, however big or small, must accurately identify the underlying features. Our approach equipped with tighter bounds on approximation errors ensures an accurate resolution in this big data setting.

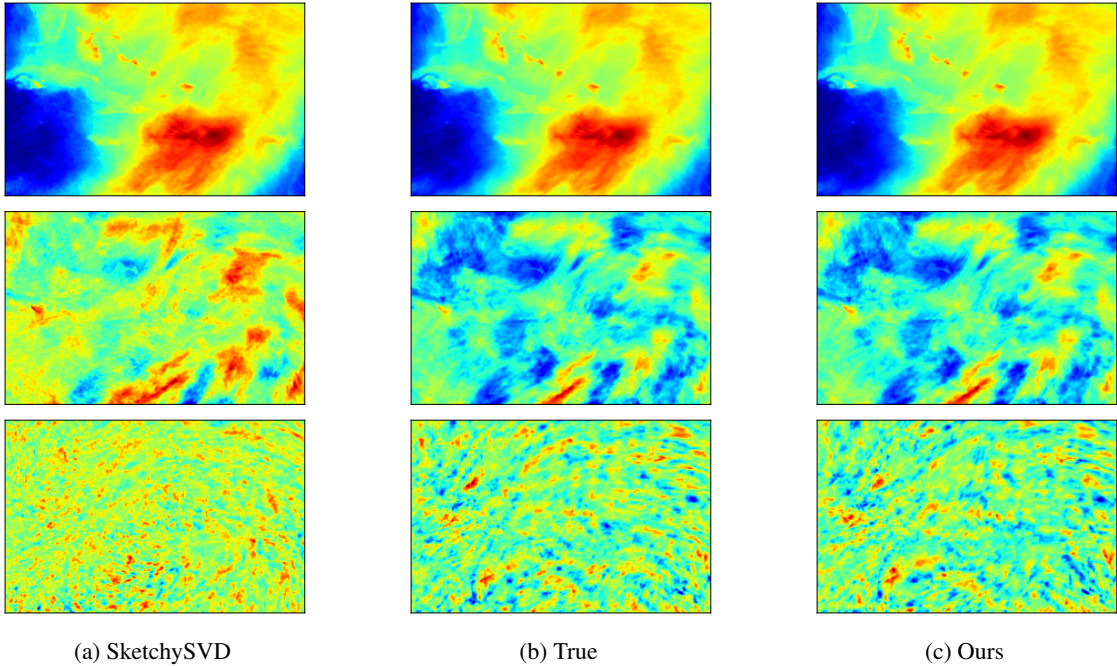


Figure 13: Reshaped U_i indicative of dynamic modes, corresponding to $i = 10, 50, 100$ for $r = 100$. The dynamic mode approximation error stands out visually for SketchySVD at indices 50, 100. Our approach compares well against the conventional SVD solution.

7 Conclusion

We present a low-weight, high-precision, fully interpretable neural SVD solver for big data applications. We show that our solution error is bounded below by the tail energy following Eckart-Young-Mirsky theorem. Our numerical experiments on real and synthetic datasets confirm these bounds. We also verify that our network minimization problem converges to this tail energy in Frobenius norm at machine precision. A number of Big Data problems are considered, where PCA, SVD, or Eigen decompositions are required, that demonstrate the applicability of the network to large scale datasets. A comparison is also provided against a state of the art randomized, streaming SVD algorithm.

References

- [1] Julio Cesar Stacchini de Souza, Tatiana Mariano Lessa Assis, and Bikash Chandra Pal. Data compression in smart distribution systems via singular value decomposition. *IEEE Transactions on Smart Grid*, 8(1):275–284, 2015.
- [2] Matthew Brand. Incremental singular value decomposition of uncertain data with missing values. In *European Conference on Computer Vision*, pages 707–720. Springer, 2002.
- [3] Shuqin Wang, Yongli Wang, Yongyong Chen, Peng Pan, Zhipeng Sun, and Guoping He. Robust pca using matrix factorization for background/foreground separation. *IEEE Access*, 6:18945–18953, 2018.
- [4] Sheng Zhang, Weihong Wang, James Ford, Fillia Makedon, and Justin Pearlman. Using singular value decomposition approximation for collaborative filtering. In *Seventh IEEE International Conference on E-Commerce Technology (CEC’05)*, pages 257–264. IEEE, 2005.
- [5] Petros Drineas, Alan Frieze, Ravi Kannan, Santosh Vempala, and V Vinay. Clustering large graphs via the singular value decomposition. *Machine learning*, 56(1-3):9–33, 2004.
- [6] Liping Jing, Chenyang Shen, Liu Yang, Jian Yu, and Michael K Ng. Multi-label classification by semi-supervised singular value decomposition. *IEEE Transactions on Image Processing*, 26(10):4612–4625, 2017.
- [7] Franco Woolfe, Edo Liberty, Vladimir Rokhlin, and Mark Tygert. A fast randomized algorithm for the approximation of matrices. *Applied and Computational Harmonic Analysis*, 25(3):335–366, 2008.
- [8] Nathan Halko, Per-Gunnar Martinsson, and Joel A Tropp. Finding structure with randomness: Probabilistic algorithms for constructing approximate matrix decompositions. *SIAM review*, 53(2):217–288, 2011.
- [9] David P Woodruff. Sketching as a tool for numerical linear algebra. *arXiv preprint arXiv:1411.4357*, 2014.
- [10] Christos Boutsidis, David P Woodruff, and Peilin Zhong. Optimal principal component analysis in distributed and streaming models. In *Proceedings of the forty-eighth annual ACM symposium on Theory of Computing*, pages 236–249, 2016.
- [11] Jalaj Upadhyay. Fast and space-optimal low-rank factorization in the streaming model with application in differential privacy. *arXiv preprint arXiv:1604.01429*, 2016.
- [12] Joel A Tropp, Alp Yurtsever, Madeleine Udell, and Volkan Cevher. Streaming low-rank matrix approximation with an application to scientific simulation. *SIAM Journal on Scientific Computing*, 41(4):A2430–A2463, 2019.
- [13] Terence D Sanger. Two iterative algorithms for computing the singular value decomposition from input/output samples. In *Advances in neural information processing systems*, pages 144–151, 1994.
- [14] Azzam Haidar, Khairul Kabir, Diana Fayad, Stanimire Tomov, and Jack Dongarra. Out of memory svd solver for big data. In *2017 IEEE High Performance Extreme Computing Conference (HPEC)*, pages 1–7. IEEE, 2017.
- [15] William B Johnson and Joram Lindenstrauss. Extensions of lipschitz mappings into a hilbert space. *Contemporary mathematics*, 26(189-206):1, 1984.
- [16] Kenneth L Clarkson and David P Woodruff. Low-rank approximation and regression in input sparsity time. *Journal of the ACM (JACM)*, 63(6):54, 2017.
- [17] Christos Boutsidis, Petros Drineas, and Malik Magdon-Ismail. Near-optimal column-based matrix reconstruction. *SIAM Journal on Computing*, 43(2):687–717, 2014.
- [18] Petros Drineas, Ravi Kannan, and Michael W Mahoney. Fast monte carlo algorithms for matrices ii: Computing a low-rank approximation to a matrix. *SIAM Journal on computing*, 36(1):158–183, 2006.
- [19] Cameron Musco and Christopher Musco. Stronger approximate singular value decomposition via the block lanczos and power methods. *arXiv preprint arXiv:1504.05477*, 16:27, 2015.
- [20] Carl Eckart and Gale Young. The approximation of one matrix by another of lower rank. *Psychometrika*, 1(3):211–218, 1936.
- [21] Leon Mirsky. Symmetric gauge functions and unitarily invariant norms. *The quarterly journal of mathematics*, 11(1):50–59, 1960.
- [22] François Chollet. keras. <https://github.com/fchollet/keras>, 2015.
- [23] Diederik P Kingma and Jimmy Ba. Adam: A method for stochastic optimization. *arXiv preprint arXiv:1412.6980*, 2014.
- [24] Gephi sample data sets. <http://wiki.gephi.org/index.php/Datasets>.
- [25] Jure Leskovec and Andrej Krevl. SNAP Datasets: Stanford large network dataset collection. <http://snap.stanford.edu/data>, June 2014.

- [26] Lev muchnik’s data sets web page. <http://www.levmuchnik.net/Content/Networks/NetworkData.html>.
- [27] James Baglama and Lothar Reichel. Augmented implicitly restarted lanczos bidiagonalization methods. *SIAM Journal on Scientific Computing*, 27(1):19–42, 2005.

A Energy Minimization and Convergence

In this section, we consider the energy minimization problem that constructs the projection space spanning the rank- r sub-space of a given data matrix. For ease of visualization, we consider a 2×2 matrix $X = \text{diag}(5, 1)$ with singular values 5 and 1 corresponding to right singular vectors $v_1 = [1, 0]^T$ and $v_2 = [0, 1]^T$, respectively. Our objective here is to extract a rank 1 approximation of this rank 2 matrix X . Certainly, this corresponds to identifying the right singular vector v_1 with singular value 5. The tail-energy surface (log-scale) corresponding to the $\|X\tilde{v}\tilde{v}^T - X\|_F$ is shown in Fig. 14. Here, \tilde{v} is the test vector for a rank 1 approximation of X . The tail-energy is a bi-quadratic function in \tilde{v} with 1 maxima, 2^r minima and 2^r saddle points, where r is the desired low-rank approximation of a given data matrix. Furthermore, all minima have the same tail energy: a property of bi-quadratic functions. For the current specific example, the two equal tail-energy minima correspond to v_1 and $-v_1$, respectively.

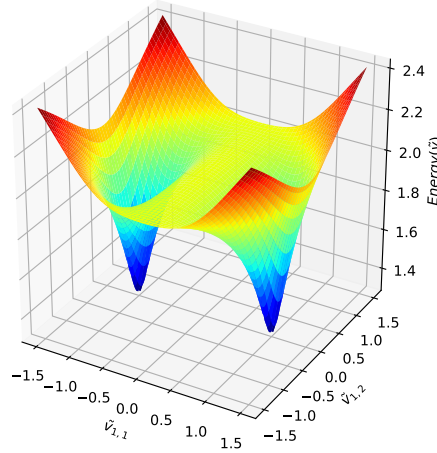


Figure 14: Surface plot for the bi-quadratic tail energy (log-scale) with 2 minima, 2 saddle points, and one maxima for $X = \text{diag}(5, 1)$.

Although the minimization problem is non-convex, convergence can be guaranteed as long as any gradient descent approach converges to either of the two minima. In other words, any test vector \tilde{v} other than v_1 or $-v_1$ will increase the tail-energy and hence will not be the solution. The same argument applies for a high-dimensional dataset X where a low rank (r) approximation is desired with the number of equal tail-energy minima corresponding to 2^r for all possible negative and positive combinations of the r right singular vectors v_i , $i = 1, \dots, r$. In effect, the stage 1 minimization problem constructs a right projection space $\tilde{V} = \text{span}\{v_1, v_2, \dots, v_r\}$ that spans the top rank- r subspace of a given dataset X . Note that according to EYM theorem, any other projection (randomized or otherwise) results in a higher tail energy leading to inaccurate singular vectors and values. In this respect, the only information preserving right projection is the one that spans the top rank- r subspace of any given data matrix. A similar line of argument then applies to our stage 2 minimization problem as well.

A mild limitation, that will be addressed in the future, occurs when $X = \text{diag}(5, 5 + \epsilon)$, $0 \leq \epsilon \ll 1$, wherein the two right singular vectors cannot be resolved accurately without further considerations. This latter case, with near algebraic multiplicity of 2 in singular values is a special case for conventional SVD. We would also like to point out that for sketchy SVD: a right projection onto an over-sampled rank, random Gaussian space results in loss of information and consequent deterioration of accuracy. Additionally, in a practical situation it is difficult to identify a priori whether a given dataset satisfies a fast decaying spectrum assumption or not. In order to identify the decay rate SVD must be performed resulting in a catch 22 for this assumption. Even if multiple, right projections are considered, convergence of the mean projection space (Central Limit Theorem) to the top- r rank sub-space of X will still require reformulation as a minimization problem with possibly an acceptance/rejection algorithm.

B Sketchy SVD Implementation

Algorithm 1 Sketchy SVD

Input: $A \in \mathbb{R}^{m \times n}$, r : expected rank

Output: $\hat{A} \in \mathbb{R}^{m \times k}$ the approximated rank k -dim data

1: Initialize $k = 4r + 1, s = 2k + 1$ 2: Projection maps: $\Upsilon \in \mathbb{R}^{k \times m}, \Omega \in \mathbb{R}^{k \times n}, \Phi \in \mathbb{R}^{s \times m}, \Psi \in \mathbb{R}^{s \times n}$ 3: Projection matrices: $X \in \mathbb{R}^{k \times n}, Y \in \mathbb{R}^{m \times k}, Z \in \mathbb{R}^{s \times s}$ as empty 4: for $i = 1 : n$ do 5: Form $H \in \mathbb{R}^{m \times n}$ as a sparse empty matrix 6: $H(i, :) = A(i, :)$ 7: $X \leftarrow X + \Upsilon H$ 8: $Y \leftarrow Y + H \Omega^T$ 9: $Z \leftarrow Z + \Phi H \Psi^T$ 10: $Q \in \mathbb{R}^{m \times k} \leftarrow qr_econ(Y)$ 11: $P \in \mathbb{R}^{n \times k} \leftarrow qr_econ(X^T)$ 12: $C \in \mathbb{R}^{k \times k} \leftarrow ((\Phi Q) \setminus Z) / (\Psi P)$ 13: $[U, \Sigma, V^T] \leftarrow svd(C)$ 14: $\Sigma \in \mathbb{R}^{r \times r} \leftarrow \Sigma[1 : r, 1 : r]$ 15: $U \in \mathbb{R}^{k \times r} \leftarrow U[:, 1 : r]$ 16: $V^T \in \mathbb{R}^{r \times k} \leftarrow V^T[1 : r, :]$ 17: $U \in \mathbb{R}^{m \times r} \leftarrow QU$ 18: $V^T \in \mathbb{R}^{r \times n} \leftarrow PV^T$ 19: $\hat{A} \in \mathbb{R}^{m \times n} \leftarrow U \Sigma V^T$	▷ Oversampling parameters ▷ Streaming Update ▷ Streamed columns ▷ Update Co-Range ▷ Update Range ▷ Update Core Sketch ▷ Basis for Range ▷ Basis for Co-Range ▷ Core Matrix ▷ Full SVD of Core Matrix ▷ Pick top r ▷ Pick top r ▷ Pick top r ▷ Project to Row Space ▷ Project to Column Space ▷ Approximation
---	---
